JBC Papers in Press. Published on June 3, 2020 as Manuscript RA120.014325
The latest version is at https://www.jbc.org/cgi/doi/10.1074/jbc.RA120.014325

The nonselective cation channel TRPV4 inhibits angiotensin II receptors

Nicholas W. Zaccor[1], Charlotte J. Sumner[1, 2], Solomon H. Snyder[1, 3, 4 *]

From the [1]The Solomon H. Snyder Department of Neuroscience, Johns Hopkins University School of Medicine, Baltimore, MD 21205; [2]Department of Neurology, Johns Hopkins University School of Medicine, Baltimore, MD 21205; [3]Department of Psychiatry and Behavioral Sciences, Johns Hopkins University School of Medicine, Baltimore, MD 21205; [4]Department of Pharmacology and Molecular Sciences, Johns Hopkins University School of Medicine, Baltimore, MD 21205

Running title: *TRPV4 inhibits angiotensin II receptors*

*To whom correspondence should be addressed: Solomon H. Snyder: The Solomon H. Snyder Department of Neuroscience, Johns Hopkins University School of Medicine, Baltimore, MD 21205; ssnyder@jhmi.edu; Tel.(410) 955-3024

Keywords: transient receptor potential vanilloid 4 (TRPV4), angiotensin II receptor type 1 (AT1R), G-protein coupled receptor, β-arrestin, phosphorylation, desensitization, calcineurin, cell signaling, cell sensor

Abstract

G protein-coupled receptors (GPCRs) are a ubiquitously expressed family of receptor proteins that regulate many physiological functions and other proteins. They act through two dissociable signaling pathways, the exchange of GDP to GTP by linked G proteins and the recruitment of β-arrestins. GPCRs modulate several members of the transient receptor potential (TRP) channel family of non-selective cation channels. How TRP channels reciprocally regulate GPCR signaling is less well explored. Here, using an array of biochemical approaches, including immunoprecipitation and -fluorescence, calcium imaging, phosphate radiolabeling, and a β-Arrestin dependent luciferase assay, we characterize a GPCR-TRP channel pair, angiotensin II receptor type 1 (AT1R) and transient receptor potential vanilloid 4 (TRPV4), in primary murine choroid plexus epithelial cells and immortalized cell lines. We found that AT1R and TRPV4 are binding partners, and that activation of AT1R by angiotensin II (ANGII) elicits β-arrestin-dependent inhibition and internalization of TRPV4. Activating TRPV4 with endogenous and synthetic agonists inhibited ANGII-mediated G-protein associated second messenger accumulation, AT1R receptor phosphorylation and β-arrestin recruitment. We also noted that TRPV4 inhibits AT1R phosphorylation by activating the calcium-activated phosphatase calcineurin in a Ca2+/calmodulin dependent manner, preventing β-arrestin recruitment and receptor internalization. These findings suggest that when TRP channels and GPCRs are co-expressed in the same tissues, many of these channels can inhibit GPCR desensitization.

Canonical GPCR signaling comprises G-protein mediated alterations in the production of the second messenger molecules cyclic-adenosine monophosphate (cAMP), inositol(1,4,5) trisphosphate (IP3) and diacylglycerol (DAG)(1). GPCRs can also signal through the recruitment of β-arrestins(2). β-Arrestins translocate to the cell membrane and bind GPCRs following ligand induced phosphorylation of the GPCR C-terminus by G-protein coupled receptor kinases (GRKs)(2, 3). β-Arrestin interactions hinder further G-protein binding, desensitize the GPCR, and also may lead to receptor internalization, recycling or degradation(2, 3). β-Arrestin also elicits G-protein independent signaling consequences through mitogen activated protein kinases (MAPKs) and serves as an adaptor protein linking GPCRs to other nearby membrane proteins(3). For example, ANGII stimulation of AT1R, can direct chemotaxis of HEK293 cells in a G-protein independent fashion, as well as induce β-arrestin dependent ubiquitination of TRPV4 ion channels in rat

vascular smooth muscle cells (rVSMC)(4, 5). Thus, β-arrestin recruitment is a critical regulatory event that dictates the signaling of GPCRs as well as other nearby proteins.

TRP channels are a large family of multimodal cation channels permeable to Ca2+, Na+ and Mg2+(6, 7). TRP channels are located in the plasma membrane of most animal cells and mediate a wide range of sensory signaling including taste, mechanosensation, osmosensation and thermosensation(7). Due to their ubiquity, TRP channels are regulated by a wide array of GPCRs. For example, AT1R activation induces catecholamine secretion from chromaffin cells by recruiting and activating transient receptor potential canonical 3 (TRPC3)(8); μ-opioid receptor (MOR1) activation inhibits cold sensation by internalizing transient receptor potential melastatin 8 (TRPM8)(9); and metabotropic glutamate receptor 1 (mGluR1) can stimulate neuronal excitatory post synaptic conductance mediated by transient receptor potential C1 (TRPC1) channels in neurons(10). A less well explored aspect of the GPCR-TRP channel interaction is the ability of TRP channels to reciprocally regulate GPCRs. We recently reported that transient receptor potential vanilloid 1 (TRPV1) can bind MOR1, inhibit MOR1 phosphorylation and block β-arrestin recruitment(11). TRPV1 activity inhibits ligand induced phosphorylation of MOR1 by GRK5 and can induce β-arrestin nuclear translocation preventing recruitment to MOR1 (11, 12).

We hypothesize that diverse GPCR-TRP channel binding partners exhibit regulatory relationships. In particular, GPCRs and TRP channels that physically bind and have antagonistic signaling consequences, such as AT1R and TRPV4, may act as reciprocal regulators. AT1R and TRPV4 are each ubiquitously expressed, but are both particularly abundant in vascular endothelial/smooth muscle cells and the choroid plexus(5, 13–16). In these cell types AT1R and TRPV4 display opposite cellular effects. In the vasculature AT1R activation stimulates vasoconstriction, whereas TRPV4 activity induces vasodilation(13, 17). In the choroid plexus AT1R and TRPV4 have similarly oppositional signaling consequences. AT1R activation stimulates the secretion of vasopressin from choroid plexus epithelial cells (CPECs) leading to diminished blood flow to the choroid plexus and decreased secretion of CSF. In contrast, TRPV4 activity increases blood flow to the choroid and increases the flux of Cl- and K+ ions into the cerebral ventricles increasing CSF production. Thus, TRPV4 and AT1R are ideally suited to regulate CSF homeostasis by regulating one another's activity.

In this study we examine whether TRPV4 and AT1R exhibit a similar regulatory relationship as TRPV1 and MOR1. We explore the ability of TRPV4 to regulate AT1R activity, phosphorylation and β-arrestin recruitment in the choroid plexus and immortalized cells and investigate how this regulatory relationship generalizes to other pairs of GPCR and TRP channels.

Results

TRPV4 physically and functionally interacts with AT1R

TRPV4 and AT1R are co-expressed in a variety of cells types including vascular endothelial cells, vascular smooth muscle cells and CPECs(5, 13, 15). Despite their co-expression in multiple tissues, TRPV4 and AT1R have only been shown to interact physically in rVSMC(5). In HEK293 cells over-expressed HA-AT1R co-immunoprecipitates (Co-IP) with Flag-TRPV4 (Fig. 1A). Treating cells with the potent TRPV4 agonist GSK101 does not affect the binding of TRPV4 to AT1R (Fig. 1A). Cultured primary murine CPECs derived from wild type (WT) mice at postnatal day 21 express endogenous TRPV4 and AT1R protein (Fig. 1B). Knockout of TRPV4 in CPECs cultured from TRPV4 null (TRPV4-KO) mice does not significantly alter AT1R expression in CPECs *in vitro* (Fig. 1B). TRPV4-KO eliminates the response of CPECs *in vitro* to 10 μM GSK101 by calcium imaging (fig. S1A). WT CPECs express mRNA for both TRPV4 (probe Trpv4) and AT1R (probe Agt1ra) (Fig. 1C). Immunoprecipitating (IP) AT1R from whole choroid plexus of WT and TRPV4-KO mice suggests that TRPV4 and AT1R bind in primary cells at endogenous expression levels (fig. S1B). AT1R is predominantly a Gαq coupled GPCR. Ligand binding to AT1R increases phospholipase C (PLC) activity, which cleaves membranous phosphatidyl inositol trisphosphate into the second messengers DAG and IP3(8, 18). To monitor IP3 production, HEK293 cells over

expressing HA-AT1R and Flag-TRPV4 were labeled with tritiated myo-inositol, and HPLC was used to separate the different phospho-inositol isoforms. ANGII stimulation of AT1R results in robust IP3 production, while pretreatment with 10 nM GSK101 for 5 min significantly inhibits IP3 production (Fig. 1D). HPLC analysis of the major phosphorylated inositol subtypes indicates that TRPV4 activation does not significantly alter levels of other phospho-inositol isoforms (fig. S1C). Additionally, we did not find evidence that TRPV4 activation by GSK101 disrupts Gαq binding to AT1R (fig. S1D).

TRPV4 inhibits AT1R phosphorylation

We next examined whether TRPV4 activity impacts ligand induced phosphorylation of a GPCR binding partner. AT1R phosphorylation, the most proximal signaling event that we can monitor, is required for AT1R mediated inhibition of TRPV4(5). HEK293 cells overexpressing HA-AT1R and Flag-TRPV4 were incubated in [32P] orthophosphate and treated with combinations of 10 nM GSK101 and 100 nM ANGII. ANGII stimulates the phosphorylation of AT1R, but TRPV4 activation prior to ANGII treatment significantly inhibits the AT1R phosphorylation (Fig. 2A). Compared to baseline, there is also a non-significant decrease in phosphorylation of AT1R when cells are treated with GSK101 alone (Fig. 2A). We did not measure AT1R phosphorylation changes in response to GSK101 when no TRPV4 was expressed. After a GPCR is phosphorylated β-arrestin is recruited to bind the GPCR C-terminus. IP of AT1R from HEK293 cells expressing Flag-TRPV4, HA-AT1R and YFP-β-arrestin after treatment with ANGII pulls down β-arrestin, which is blocked by pre-treatment with GSK101 (Fig. 2B).

We employed the luciferase-based TANGO system to explore details of β-arrestin recruitment to AT1R. The TANGO system leverages an engineered HEK293 cell line (HTLA) that produces the luciferase enzyme following β-arrestin translocation to the cell membrane and binding to a GPCR(19). Activation of AT1R with 100 nM and 1 μM ANGII significantly increases β-arrestin recruitment to AT1R, which is blocked by TRPV4 activation with 10 nM GSK101 (Fig. 2C). The endogenous TRPV4 agonist 11,12-epoxyeicosatrienoic acid (11,12-EET) also inhibits β-arrestin recruitment to AT1R (fig. S2A)(20). Interestingly, 10 nM GSK101 alone is sufficient to significantly decrease β-arrestin recruitment and luciferase production compared to baseline which could indicate a reduction in ligand independent phosphorylation (Fig. 2C). To determine whether our assay was measuring a reduction in ligand independent phosphorylation we treated HTLA cells with olmesartan, an inverse agonist of AT1R. Applying 5 nM olmesartan to HLTA cells expressing AT1R is sufficient to block β-arrestin recruitment but does not lower baseline luciferase production (fig. S2B). Stimulating TRPV4 with increasing concentrations of GSK101 causes a dose responsive decrease in the amount of β-arrestin recruitment to AT1R with an approximate IC50 between 0.5 and 1 nM (Fig. 2D). GSK101 has no effect when TRPV4 is not expressed (fig. S2C). Preincubation of cells with the TRPV4 antagonist HC067 (Fig. 2E) and ruthenium red another TRP channel antagonist dose dependently rescues ANGII stimulated β-arrestin recruitment to AT1R (fig. S2D,E). Taken together this data indicates TRPV4 activation is necessary to block ligand induced binding of β-arrestin to AT1R.

TRPV4 activates the phosphatase calcineurin to dephosphorylate AT1R

Protein phosphorylation can be regulated by two mechanisms, the initial phosphorylation by a protein kinase, and the dephosphorylation by a protein phosphatase. TRPV1 inhibits MOR1 phosphorylation by stimulating the nuclear translocation of G-protein coupled receptor kinase 5 (GRK5)(11). TRPV4 activation can also induce the translocation of GRK5 out of the plasma membrane (fig. S3A). We performed an order-of-addition experiment to determine if TRPV4 regulates AT1R phosphorylation by inhibiting a protein kinase, such as GRK5, or activates a protein phosphatase. If TRPV4 inhibits a kinase, then reversing the order in which TRPV4 and AT1R are activated will produce different results, because once a kinase has completed phosphorylation of a substrate, it does not matter if it is inhibited. Conversely, if TRPV4 activates a phosphatase, the order in which TRPV4 and AT1R are activated is irrelevant, because the phosphatase will immediately dephosphorylate its substrate. The

order in which TRPV4 and AT1R are activated has no significant effect on TRPV4 mediated inhibition of β-arrestin recruitment (Fig. 3A). This suggests that TRPV4 inhibits AT1R phosphorylation by activating a protein phosphatase.

Calcineurin is a Ca2+/calmodulin activated protein phosphatase that can be activated by TRPV4(21, 22). Furthermore, calcineurin can inhibit the desensitization of 5-HT1c receptors, a GPCR expressed in the choroid plexus(23, 24). Incubating HTLA cells transiently transfected with TRPV4 and AT1R in 30 μM of a cell permeable calcineurin autoinhibitory peptide (CAP) blocks TRPV4 inhibition of β-arrestin recruitment (Fig. 3B). CAP rescues β-arrestin binding in a dose responsive manner with an approximate EC50 ~1.2 μM (Fig. 3C). Phosphorylated nuclear factor of activated T-cells (p-NFAT) is the canonical target of calcineurin dephosphorylation(25). Activated calcineurin dephosphorylates p-NFAT and initiates NFAT translocation from the cytoplasm to the nucleus(25). Activating TRPV4 in HEK293 cells with 10 nM GSK101 is sufficient to significantly dephosphorylate p-NFAT, and reduce NFATC1 in the cytoplasm (Fig. 3D, fig. S3B). There is no significant change of NFATC1 in the nucleus (Fig. 3D). Incubating HEK293 cells expressing TRPV4 in 30 μM CAP blocks TRPV4 mediated p-NFAT dephosphorylation (Fig. 3D). We found inhibiting calcineurin completely blocks the effects of TRPV4 on β-arrestin recruitment. We wondered whether other phosphatases are activated by TRPV4. Incubation of cells in 100 nM okadaic acid, a broad phosphatase inhibitor that does not block calcineurin, does not recapitulate the effects of inhibiting calcineurin (Fig. 3E)(26). Furthermore, calcineurin activation requires calmodulin(25, 27). Consequently, culturing HTLA cells in calmidazolium, a calmodulin inhibitor, similarly prevents TRPV4 from blocking β-arrestin recruitment to AT1R in a dose dependent manner, EC50 ~3μM (Fig. 3F). Taken together, the results demonstrate that TRPV4 specifically activates calcineurin in a Ca2+/calmodulin dependent manner which is sufficient to dephosphorylate AT1R and block β-arrestin recruitment.

TRPV4 and TRPV1 both can inhibit phosphorylation of GPCRs that are in close proximity in a Ca2+/calmodulin dependent manner. It is likely that many other TRP channels similarly regulate nearby GPCRs. Co-expressing and activating TRPV1 by capsaicin, (Fig. 3G) and TRPA1 by iodoacetamide (IA) (fig. S3C) with AT1R both block ANGII stimulated β-arrestin recruitment. Similarly, when TRPV4 is co-expressed with another GPCR, mas-related G-protein coupled receptor membrane A1 (MRGA1), GSK101 stimulation blocks β-arrestin recruitment to MRGA1 stimulated with Phe-Met-Arg-Phe-amide (FMRF) (fig. S3D). Previous work demonstrated that TRPV1 inhibits phosphorylation of MOR1 by inhibiting a kinase(11). Incubating TRPV1 and AT1R expressing cells with CAP does not rescue TRPV1 mediated inhibition of β-arrestin recruitment (Fig. 3H). Taken together our findings reveal that diverse TRP channels inhibit GPCR phosphorylation but may do so via distinct molecular pathways for different TRP channels.

TRPV4 activity is regulated by AT1R activation

The choroid plexus is a tissue where TRPV4 and AT1R are likely to regulate each other's activity. TRPV4 and AT1R have opposite roles in regulating blood flow to the choroid plexus and in the production of CSF(13, 15, 17, 28). To test whether AT1R activation can inhibit TRPV4 in cells other than vascular smooth muscle cells(5) we used to CPECs as a model tissue for TRPV4-AT1R reciprocal regulation. Primary murine CPECs exposed to 100 nM ANGII *in vitro* have significantly reduced calcium inflows in response to GSK101 treatment (Fig. 4A). Calcium influx in CPECs induced by GSK101 is specific to TRPV4 activation and is completely blocked when CPECs are incubated in GSK205, a TRPV4 specific antagonist (Fig. 4A). AT1R inhibits TRPV4 by recruiting β-arrestin(5). We found that activating TRPV4 before AT1R blocks recruitment of β-arrestin to AT1R. Therefore, TRPV4 can prevent its own inhibition. Accordingly, calcium imaging of CPECs that were incubated in GSK101 before treating the cells with ANGII partially rescues TRPV4 mediated calcium influx in response to further GSK101 treatment (Fig. 4B).

Activation of GPCRs results in β-arrestin-mediated receptor internalization(2, 3). We performed non-permeabilized IF of HEK293 cells transiently transfected with HA-AT1R and Flag-TRPV4 to examine changes in AT1R localization following stimulation with ANGII and GSK101. At

baseline AT1R is largely restricted to the cell membrane (Fig. 4C top left), but when treated with ANGII, it undergoes robust internalization (Fig. 4C top right). GSK101 treatment alone does not influence membrane localization of AT1R (Fig. 4C bottom left). Treating cells with GSK101 prior to the application of ANGII largely prevents AT1R internalization (Fig. 4C bottom right). This result implies β-arrestin is only recruited to the membrane when ANGII is given alone. IF of β-arrestin shows only recruited to the cell membrane (fig. S4A) when HEK293 cells expressing AT1R and TRPV4 are treated with ANGII, and not when cells are treated with the combination of GSK101 and ANGII (fig. S4A). In summary, TRPV4 and AT1R can both regulate one another's activity/signaling as well as their membrane localization (a summary of the interaction is shown in Fig. 4D).

Discussion

Our study reveals that TRPV4 and AT1R reciprocally interact in the choroid plexus and that TRPV4 activity can inhibit AT1R signaling. Activation of TRPV4 stimulates the protein phosphatase calcineurin, which dephosphorylates AT1R, inhibiting the β-arrestin mediated internalization of AT1R. TRPV4 activation also appears to decrease AT1R Gαq signaling by reducing ANGII stimulated IP3 production. Notably, the regulatory mechanism we describe here likely generalizes to other pairs of TRP channels and GPCRs. Our study expands on the underappreciated role that TRP channel activity has in reciprocally regulating the activity, localization and sensitization of GPCRs.

Co-IP studies in HEK293 cells and primary CPECs suggest that TRPV4 and AT1R are binding partners or interact in a macromolecular complex (Fig. 1A, fig. S1B). This reinforces prior evidence that endogenous TRPV4 and AT1R bind in rat vascular smooth muscle cells(5). Shukla and colleagues showed that AT1R stimulation by ANGII causes β-arrestin dependent ubiquitination and functional inhibition of TRPV4 by AIP4 (an E3-ubiquitin ligase) (Fig. 4C middle)(5). Analogously, in our study exposure of CPECs to ANGII inhibits TRPV4 responses to GSK101 (Fig. 4A). Interestingly there are other proteins that are activated by ANGII such as Mas1 and angiotensin receptor type 2 that may also be able to interact with TRPV4 in the choroid plexus. GPCRs can regulate TRP channels through a variety of mechanisms including direct G-protein mediated activation(8, 29), allosteric sensitization(30), inhibition by internalization(5), removal of inhibition(31) and inhibition of sensitization(32). The potential for TRP channels to regulate GPCRs has been examined far less.

Our results provide converging physiologic and pharmacologic evidence that TRP channels are important regulators of GPCR signaling, phosphorylation, β-arrestin recruitment and GPCR internalization. The exact mechanism by which TRPV4 inhibits Gαq signaling is not known. We found no compelling evidence that TRPV4 activity interrupts G-protein GPCR coupling (fig. S1D). We did however notice in our HPLC experiments that TRPV4 activation seemed to increase the accumulation of IP1 (Fig. S1C). The enzyme responsible for degrading IP3 to IP1 is polyphosphate 5-phosphatase (P5P). The rate of P5P conversion of IP3 to IP1 is increased in the presence of increasing Ca2+ and elevated protein kinase C (PKC) activity(33). Therefore, TRPV4 may not be directly inhibiting Gαq signaling, but rather decreasing the accumulation of the second messenger IP3. The ability of TRPV4 to inhibit AT1R Gαq signaling contrasts with our work with TRPV1 and MOR1, wherein TRPV1 had no influence on MOR1 mediated Gαi signaling(11). A limitation of this experiment is we did not assay the production of IP3 in the absence of TRPV4 when cells were still treated with GSK101. Therefore, we did not control for potential off target effects GSK101 may have on downstream AT1R signaling. However, given that GSK101 does not affect calcium signaling in TRPV4 knockout cells (fig. S1B) and has no effect on β-arrestin recruitment to AT1R in untransfected HEK293 (fig. S2C) we do not believe those off-target effects significantly affect our conclusions.

TRP channels can inhibit GPCR phosphorylation and regulate β-arrestin localization(11, 12). In contrast to TRPV1, which inhibits the phosphorylation of MOR1 by GRK5, TRPV4 activates calcineurin to dephosphorylate AT1R. TRPV4 activates calcineurin in a Ca2+/calmodulin dependent manner in osteoclasts, airway smooth muscles cells and skeletal muscle(21, 22, 34). Our results indicate TRPV4 can

stimulate calcineurin activity in a wide range of tissues including the choroid plexus. Calcineurin canonically signals by stimulating the nuclear translocation of NFAT, which induces cell type specific changes in gene transcription(25). Calcineurin can also inhibit the desensitization of GPCRs(23, 35). Thus, TRPV4 not only directs calcineurin to dephosphorylate AT1R, but may also drive NFAT dependent transcriptional changes in many tissues. An important caveat to this is our results did not show a significant increase of NFAT in the nucleus, only decreased pNFAT in the cytoplasm (Fig. 3D).

Our findings suggest that many TRP channels can regulate GPCR phosphorylation, though not necessarily by activating calcineurin. When TRPA1 and TRPV1 were artificially expressed with AT1R, both proteins could inhibit ligand induced receptor phosphorylation. Additionally, when TRPV4 was transiently expressed with MRGA1 it was similarly able to inhibit MRGA1 phosphorylation. It is possible that we randomly selected special GPCR-TRP pairs, but more likely that many pairs of GPCR-TRP channels exhibit an equivalent regulatory relationship. The specificity of the regulation is likely determined by the cell type being studied and whether the TRP channel and GPCR of interest physically interact. Interestingly, though activating TRPV1 and TRPV4 leads to an equivalent functional outcome on AT1R phosphorylation, the result is achieved through molecularly distinct signaling mechanisms (Fig. 3 B, H).

Whether a GPCR-TRP channel pair are physiologically important regulators likely depends on their tissue expression profiles. TRPV4 and AT1R are co-expressed in many of tissues, but in the vasculature and the choroid plexus they elicit opposite signaling outcomes making them potential reciprocal regulators. In the vasculature AT1R is a vasoconstrictor and TRPV4 is a vasodilator. Crosstalk between the two proteins may be essential for maintenance of appropriate vascular tone(5, 13). Under physiologic conditions AT1R and TRPV4 interact in the choroid plexus to maintain homeostatic rates of CSF production on a minute to minute time scale. CPECs produce ~80% of cerebrospinal fluid (CSF) and express all the molecular components of the renin-angiotensin-aldosterone system(28, 36). When intraventricular ANGII binds AT1R, CPECs secrete arginine vasopressin which results in reduced blood flow to the choroid plexus, and diminished Cl- efflux into the cerebral ventricles(28). The net effect of AT1R signaling is decreased CSF production. Conversely, activating TRPV4, which functions as an osmolarity sensor in the choroid plexus, increases Cl- and K+ efflux through calcium-activated chloride/potassium channels resulting in enhanced CSF production(15, 37). TRPV4 and AT1R are uniquely situated as a GPCR-TRP channel pair to regulate each other's activity and localization and maintain homeostatic CSF production.

In summary, we have demonstrated a novel mechanism for TRPV4 to inhibit AT1R receptor phosphorylation and activity. Calcium influx through TRPV4 leads to the Ca2+/calmodulin dependent activation of calcineurin, and subsequent dephosphorylation of AT1R. This interaction is not only important for the regulation of AT1R activity, but also relieves AT1R mediated inhibition of TRPV4. Our evidence indicates that this regulatory pathway is likely conserved across other GPCR-TRP channel pairs. Our model suggests that other pairs, such as TRPC1-dopamine receptor D2 and TRPM8-serotonin receptor 1B would be good targets to examine and expand our understanding this regulatory pathway as they are already known to interact physically and physiologically(30, 38). Given the broad expression of TRP channels and the medical importance of GPCRs, it is possible that TRP channel agonists will have therapeutic potential as modulators of GPCR activity, desensitization and localization.

Experimental procedures

Drugs/Chemicals

Chemicals used to generate buffers were purchased from Sigma unless otherwise indicated. Concentrations of drugs used is indicated in the text and figure legends. GSK1016790A (Sigma G0798), Angiotensin II (Sigma A9525), EGTA (Sigma 03777), Calcineurin Autoinhibitory Peptide (Millipore 207001), Ruthenium Red (Sigma R2751), HC067047 (Sigma SML0143), 11,12 EET (Cayman Chemical 50511), Calmidazolium chloride (Sigma C3930), Okadaic Acid (Abcam ab120375), Iodoacetamide (Sigma I1149), FMRF (Sigma N3637), PhosSTOP (Sigma 4906845001), Protease inhibitor cocktail (P8340).

Cell culture and transfection

HEK293 cells were grown in regular Dulbecco's Modified Eagle Medium supplemented with 10% fetal bovine serum (FBS, Sigma), 2mM Glutamine (Invitrogen) and 1000 units Penicillin/Streptomycin (Invitrogen). Where serum free media is indicated no FBS was supplemented to DMEM. Primary choroid plexus epithelial cells were cultured in regular DMEM supplemented with EGF 100ng/mL (Sigma) and AraC 20 μM (Sigma). HTLA cells were maintained in regular DMEM supplemented with hygromycin 1ug/mL (Invivogen) and puromycin 3ug/mL (Gibco) and were generously donated by Bryan Roth(19).

Cells were transfected using Lipofectamine 3000 (Invitrogen) according to company provided protocol. Wild type HA-AT1R was generated by site directed mutagenesis using Quikchange/Stratagene techniques from pcDNA3.1 AT1R DRY-AAY (rat), which was a gift from Laszlo Hunyady & Robert Lefkowitz (Addgene plasmid # 45759)(39). Flag-TRPV4 (human) construct has been previously described. TRPV4 cDNA was provided by Miguel Angel Valverde(40). The MRGA1 construct has been previously described(41) and was cloned into the Tango vector (a gift from Bryan Roth) using standard techniques. AT1R-Tango (human) construct was a gift from Bryan Roth (Addgene plasmid # 66222)(19). YFP-β arrestin 1 (rat) was a gift from Robert Lefkowitz (Addgene plasmid #36916)(42). GFP-Gαq (mouse) was a gift from Catherine Berlot (Addgene plasmid #66080)(43). TRPV1 cDNA and TRPA1 cDNA (gifts from Michael Caterina), pWZL Neo Myr Flag GRK5 (human) was a gift from William Hahn & Jean Zhao (Addgene plasmid # 20495)(44), were inserted into p3xFLAG-CMV-7 (Sigma) by standard cloning methods.

Western blotting

Cells were lysed in lysis buffer (20 mM Tris-HCl [pH 7.4], 140 mM NaCl, 1% IPEGAL 630) supplemented with a complete protease inhibitor cocktail (Roche) and phosphatase inhibitor tablet (Roche) on ice, unless otherwise indicated. Lysate protein content was determined using Bradford reagent (Sigma). Lysates were boiled in 1×NuPAGE lithium dodecyl sulfate sample buffer (Invitrogen) and subjected to SDS-PAGE using the Novex system (Invitrogen) following manufacturer's instructions, transferred to PVDF membranes (Millipore), blocked in 3% bovine serum albumin (Sigma) in Tris-buffered saline/0.1% Tween-20 for 1 h at room temperature, and incubated with primary antibodies overnight at 4°C. In figures containing multiple Western blot panels, triplicate gels were run containing equivalent samples.

Antibodies used were Na+/K+ ATPase (DSHB a6f) 1:1000, FLAG M2 (Sigma F3165) 1:2000, HA (Roche 11867423001) 1:1000, 12CA5 HA antibody (Roche 11583816001), TRPV4 (Abcam ab39260) 1:1000, AT1R1 (Abcam ab18801) 1:1000, Phospho-NFATC1 (R&D MAB5640) 1:1000, NFAT1 (CST 4389S) 1:1000, GFP (Abcam ab290) 1:1000, myc 9E10 (Roche 11667203001) 1:1000, GRK5 (Santa Cruz sc-565) 1:1000, Amersham ECL Mouse IgG HRP-linked (GE NA931) 1:10000, and Amersham ECL Rabbit IgG HRP-linked (GE NA934) 1:10000, Rat IgG HRP-linked (CST 7077S) 1:1000.

Immunoprecipitation

Co-immunoprecipitation experiments were performed using EZview Red Flag-agarose (Sigma) for Flag-tagged constructs and Protein A/G agarose (EMD Millipore) for HA-tagged, and endogenous protein pulldowns. The ratio of primary antibody:agarose beads was 5ug:40uL. Lysis buffer for immunoprecipitation experiments was same as for western experiments unless otherwise noted. Protease inhibitor cocktail (sigma) and PhosphoSTOP tablets (Roche) were added on the day of cells lysis. Protein content was determined using Bradford reagent (Sigma). Equal amounts of protein were added to beads and 25ug of protein was kept for input gels. Lysates incubated with beads over night at 4C and were washed 3x in lysis buffer before protein was eluted and run on SDS-page gel. Lysis buffer for β-arrestin immunoprecipitation experiments consisted of 5mM HEPES, 0.5% NP-40, 250mM NaCl, 2mM EDTA 10% v/v Glycerol.

HPLC and Inositol Triphosphate Measurement

HEK293 cells were plated in 6-well plate and transfected with HA-AT1R and Flag-TRPV4. Media was supplemented with 40uCi of [3H] D-

myoinositol (Perkin Elmer) 6 hrs after transfection. After 48 hours media was exchange for serum free media and cells were incubated at 37C for 2 hrs. Cells were than washed with Hanks Balanced Salt Solution (HBSS, Gibco) 3x, and then allowed to incubate in HBSS supplemented with 20mM LiCl for 20minutes. Combinations of 10nM GSK101 and 100nM ANGII were added for 5 min and 2 min respectively. Cells were lysed with 200ul of lysis solution, 0.6M perchloric acid (Sigma), 0.2mg/ml phytic acid (Sigma), 2mM EDTA. Cell plates were then allowed to sit at -80C for 10 min. Lysates were neutralized with 30ul 1M K2CO3. Lysates were collected and shaken overnight at 4C. Supernatants were run over a PARTiSPHERE SAX 5 micron HPLC column and collected in ninety 1 minute fractions. Ultimo-Flo AP scintillation fluid was added to each fraction and the radioactivity was measured using a LS 6500 Multi-Purpose Scintillation Counter (Beckman Coulter).

Tango-Luciferase

The Tango-luciferase system has been described in detail previously [Bryan Roth]. Briefly, Cells were plated in a 24-well plated transfected with AT1R-Tango and Flag-TRPV4. After 48 hrs media was exchanged for serum free media and the cells were allowed to incubate for 4 hours. Cells were then incubated with drug combinations mentioned in the text. TRP channel agonist were applied for 10 min and GPCR agonists were applied for 30 minutes. After drug treatments, the media was exchanged for serum free DMEM and cells were incubated at 37C for 6 hours. Cells were lysed with 100uL passive lysis buffer (Promega E194A) containing protease inhibitor cocktail. Lysates were spun down and then 10ul of each supernatant was combined with 10 ul Bright-Glo (Promega E2610). Luminescence was measured and integrated of 10 secs with a TD-20/20 Luminometer (Turner Designs).

Animal Protocol and Primary Cell Collection

Three-Four-week-old C57BL/6 male/female mice (Jackson Labs) were used for all the animal-based experiments unless otherwise indicated. TRPV4-KO mice have been previously described and were obtained through Makoto Suzuki(45). Animal breeding and procedures were conducted in strict accordance with the NIH Guide for the Care and Use of Laboratory Animals. Animal experiments were approved by the Johns Hopkins University Animal Care and Use Committee. Animals were kept on a 12 h light/dark cycle and were provided food and water ad libitum.

Extensive protocols for culture of primary mouse CPECs have been published(24, 46). Briefly, mice were euthanized by cervical dislocation, rapidly decapitated and the brain was placed in HBSS. The whole choroid plexus was dissected from both the lateral and the fourth ventricles. The choroid plexus from multiple mice of the same genotype were pooled and digested using 0.25% trypsin for 20 min. Following digestion cells were plated on 35mm glass culture dishes (MatTek) precoated with 0.1% collagen. Cells were cultured for 12 days with media exchanges every three days. Media contained 10 ng/mL epidermal growth factor (Sigma) and cytosine arabinoside 20 μM (Sigma).

Calcium imaging

CPEC cultured for 12 days *in vitro* on 0.1% collagen precoated MatTek 35mm dishes. 24 hours prior to imaging regular media was exchanged for serum free media. Cells were treated with 5ul of Fura-2 AM in 95% DMSO, 5% pluronic acid for 40 minutes prior to imaging. Cells were imaged every 5 seconds with (40-160)ms 340nm exposure and (200-800)ms 380nm exposure. Final ratiometric data was background subtracted and analyzed for drawn regions of interest that covered the entire cell.

Immunofluorescence/Whole Mount

HEK293 cells were plated on 35mm MatTek dishes precoated with poly-l-ornithine (Sigma), and transiently transfected with Flag-TRPV4 and HA-AT1R. After 24 hours media was exchanged for serum free media and cells were incubated for 24 more hours. For AT1R internalization experiments primary antibody (HA Roche 11867423001, 1:100) was added prior to permeabilization and drug treatments. For β-arrestin staining primary antibody (GFP Abcam ab290, 100) was added after permeabilization and drug treatments. Cells were incubated in blocking buffer 0.1% BSA in PBS for 30 min at 4°C and then incubate with primary antibody for 1 hr at 4°C. HEK293 cells were then fixed with 4% paraformaldehyde in PBS (Electron Microscopy

Sciences) for 15 minutes. Cells were washed 2x in PBS and permeabilized in 0.1% Triton X-100 in PBS for 15 min. Cells washed 3x in PBS and the blocked for 45 min at room temperature in 0.1% BSA 0.3% Milk in Tris-Buffered Saline pH 7.4. Cells were then then incubated in secondary antibody (1:1000) for 1 hour at room temperature. Hoechst (Sigma) added for the last 3 minutes of secondary antibody incubation. Cells washed 3x and then sealed with Vectashield HardSet mounting media (Vectorlabs).

Cell fractionation

Cell fractionation and cytoplasm and crude membrane cell compartments were isolated per our published protocol(47). Briefly, HEK293 cells expressing proteins of interest were collected from 60mm culture dishes, pelleted cells and snap frozen in buffer 1 (Buffer 1: 10 mM HEPES pH 7.4, 1 mM EGTA, 1 mM dithioreitol (DTT), 10% sucrose, protease and phosphatase inhibitors (Roche)). Pellets were centrifuged at 1000g for 10 minutes, save supernatant, re-homogenize pellet in buffer 1, spin at 1000g for 10 minutes at 4°C, save and combine supernatants. Supernatants contain crude membrane and cytoplasm, nuclear protein have been removed. Centrifuge combined supernatants at 11,000g for 20 minutes at 4°C. Supernatant contains cytoplasmic proteins, the pellet contains crude membrane. Pellet resuspended in buffer 2 (Buffer 2: 10 mM HEPES pH 7.4, 1 mM EGTA, 1 mM DTT, 1 mM $MgCl_2$), and centrifuged at 21,000g for 20 minutes at 4°C. Final pelleted resuspended in 40ul buffer 2. Proteins were separated by SDS-Page and immune blotted for proteins of interest.

Radioactive Phosphate Labeling

A detailed protocol on radiolabeling GPCRs with hot phosphate has been previously described(48). Briefly, HEK293 cells were transfect in with HA-AT1R and Flag-TRPV4 as indicated above. The cells were cultured overnight in serum free media and then incubated in phosphate free media supplemented with [32P] orthophosphate (Perkin Elmer). Cells were treated with combinations of 10nM GSK101 for 5 minutes and 100nM ANGII for 10 minutes. Cells were lysed with 300ul lysis buffer containing 50 mM Tris-HCl pH 7.5, 150 mM NaCl, 4 mg/mL n-dodecyl m-maltoside (Sigma) and 0.5 mg/mL cholesteryl hemisuccinate (Sigma), protease inhibitor cocktail (Sigma), 10mM sodium fluoride (Sigma), 4.5mg/mL sodium pyrophosphate, 0.5uM okadaic acid (Abcam). Protein was pulled down on protein-A agarose (Roche) with 12CA5 anti-HA antibody (Roche). Beads were washed 3x in various salt solutions. 30ul of sample was added per lane. SDS-Page separation was performed as indicated above. Gels were dried on vacuum gel drier for 1 hr. Dried gel was exposed to a storage phosphor screen (Molecular Dynamics) for 1 hr and imaged on a Typhoon FLA9500 (GE) with a 635nM laser, 800V PMT and 100um pixel scanning. Lane intensity was measured in the ImageJ (NIH) software package.

RT-qPCR

Taqman RNA-to-CT 1-Step (Applied biosystems 4392938) was used for all mRNA measurement. RNA was collected using RNeasy Mini Kit (Qiagen 74104). RT-qPCR was performed with a Step One Plus Real Time PCR system (Applied Biosystems) according to company guidelines. All primers were obtained from Thermo Fisher Scientific: Trpv4 (Mm00499025), Agt1ra (Mm00507771), Hprt (Mm00446968), and ActB (Mm00607939). All probes are exon spanning.

Statistics and image analysis

Western blot image analysis/densitometry was performed in ImageJ (NIH). Immunofluorescence images were contrast enhanced to improve image visibility, all contrast changes were performed uniformly across the image and no quantitative analysis was performed on any contrast modified image. Densitometry measurements were normalized to loading proteins for each cellular compartment: GAPDH for cytoplasmic proteins and Histone 2B for nuclear compartment. The no treatment group was used to standardize across blots and set to a density of 1. Graphs and statistics were performed in the statistics and graphing program Prism 8. Dose response curve lines of fit were calculated by normalizing the data to a dose of zero, and curve fitting with a 4-variable non-linear regression. Estimated EC50 and IC50 values were calculated by the best line of fit. All luciferase production experiments were normalized to total protein per sample (luminescence/[total protein]). When graphed luciferase experiments were normalized to the no treatment condition so that control = 100%.

Unless otherwise indicated a one-way ANOVA corrected for multiple comparisons and a post hoc Tukey test were performed to judge statistical significance. A significant result was considered $p<0.05$.

Data Availability Statement:
All data used in generation of this manuscript are presented in the main text and supplemental materials. Requests for more information can be directed to the corresponding author: Dr. Solomon Snyder, ssnyder@jhmi.edu

Acknowledgements:
We thank Dr. Jeremy Nathans (Johns Hopkins University School of Medicine) for access to his luminometer. We thank Dr. Rachel Green (Johns Hopkins University School of Medicine) for access to her Typhoon phosphor imaging system. We also thank Roxanne Barrow (Johns Hopkins University) and Adele Snowman (Johns Hopkins University) for their assistance with the molecular biology and construct cloning. We lastly thank Chirag Vasavda, Jeremy Sullivan, William Aisenberg and Daniel Ramos (Johns Hopkins University School of Medicine) for their helpful discussions.

Conflicts of Interest:
All of the authors listed certify that they have no affiliations with or involvement in any organization or entity with any financial or non-financial interest in the subject matter or materials discussed in this article.

Contributions:
N.W.Z, C.J.S and S.H.S participated in experiment design and data analysis. N.W.Z performed the experiments. N.W.Z, C.J.S and S.H.S wrote the manuscript.

References:

1. Gilman,A.G. (1987) G Proteins: Transducers of Receptor-Generated Signals. *Annu. Rev. Biochem.*, **56**, 615–649.
https://doi.org/10.1146/annurev.bi.56.070187.003151

2. Hilger,D., Masureel,M. and Kobilka,B.K. (2018) Structure and dynamics of GPCR signaling complexes. *Nat. Struct. Mol. Biol.*, **25**, 4–12.
https://doi.org/10.1038/s41594-017-0011-7

3. Wisler,J.W., Xiao,K., Thomsen,A.R. and Lefkowitz,R.J. (2014) Recent developments in biased agonism. *Curr. Opin. Cell Biol.*, **27**, 18–24.
https://doi.org/10.1016/J.CEB.2013.10.008

4. Hunton,D.L., Barnes,W.G., Kim,J., Ren,X.-R., Violin,J.D., Reiter,E., Milligan,G., Patel,D.D. and Lefkowitz,R.J. (2005) -Arrestin 2-Dependent Angiotensin II Type 1A Receptor-Mediated Pathway of Chemotaxis. *Mol. Pharmacol.*, **67**, 1229–1236.
https://doi.org/10.1124/mol.104.006270
http://www.ncbi.nlm.nih.gov/pubmed/15635042

5. Shukla,A.K., Kim,J., Ahn,S., Xiao,K., Shenoy,S.K., Liedtke,W. and Lefkowitz,R.J. (2010) Arresting a Transient Receptor Potential (TRP) Channel. *J. Biol. Chem.*, **285**, 30115–30125.
https://doi.org/10.1074/jbc.M110.141549
http://www.ncbi.nlm.nih.gov/pubmed/20650893

6. Zheng,J. (2013) Molecular mechanism of TRP channels. *Compr. Physiol.*, **3**, 221–42.
https://doi.org/10.1002/cphy.c120001
http://www.ncbi.nlm.nih.gov/pubmed/23720286

7. Luft,F.C. (2015) Tripping out on TRPV4. *J. Mol. Med.*, **93**, 1283–1285.
https://doi.org/10.1007/s00109-015-1347-2
http://www.ncbi.nlm.nih.gov/pubmed/26498124

8. Liu,C.-H., Gong,Z., Liang,Z.-L., Liu,Z.-X., Yang,F., Sun,Y.-J., Ma,M.-L., Wang,Y.-J., Ji,C.-R., Wang,Y.-H., *et al.* (2017) Arrestin-biased AT1R agonism induces acute catecholamine secretion through TRPC3 coupling. *Nat. Commun.*, **8**, 14335.
https://doi.org/10.1038/ncomms14335

9. Shapovalov,G., Gkika,D., Devilliers,M., Kondratskyi,A., Gordienko,D., Busserolles,J., Bokhobza,A., Eschalier,A., Skryma,R. and Prevarskaya,N. (2013) Opiates Modulate Thermosensation by Internalizing Cold Receptor TRPM8. *Cell Rep.*, **4**, 504–515.
https://doi.org/10.1016/j.celrep.2013.07.002
http://www.ncbi.nlm.nih.gov/pubmed/23911290

10. Kim,S.J., Kim,Y.S., Yuan,J.P., Petralia,R.S., Worley,P.F. and Linden,D.J. (2003) Activation of the TRPC1 cation channel by metabotropic glutamate receptor mGluR1. *Nature*, **426**, 285–291.
https://doi.org/10.1038/nature02162

11. Scherer,P.C., Zaccor,N.W., Neumann,N.M., Vasavda,C., Barrow,R., Ewald,A.J., Rao,F., Sumner,C.J. and Snyder,S.H. (2017) TRPV1 is a physiological regulator of μ-opioid receptors. *Proc. Natl. Acad. Sci. U. S. A.*, **114**.

https://doi.org/10.1073/pnas.1717005114

12. Basso,L., Aboushousha,R., Fan,C.Y., Iftinca,M., Melo,H., Flynn,R., Agosti,F., Hollenberg,M., Thompson,R.J., Bourinet,E., *et al.* (2018) TRPV1 regulates opioid analgesia during inflammation. *bioRxiv*, 10.1101/274233.
https://doi.org/10.1101/274233

13. Filosa,J.A., Yao,X. and Rath,G. (2013) TRPV4 and the regulation of vascular tone. *J. Cardiovasc. Pharmacol.*, **61**, 113–9.
https://doi.org/10.1097/FJC.0b013e318279ba42
http://www.ncbi.nlm.nih.gov/pubmed/23107877

14. Millar,I.D., Bruce,J.I. and Brown,P.D. (2007) Ion channel diversity, channel expression and function in the choroid plexuses. *Cerebrospinal Fluid Res.*, **4**, 8.
https://doi.org/10.1186/1743-8454-4-8
http://www.ncbi.nlm.nih.gov/pubmed/17883837

15. Takayama,Y., Shibasaki,K., Suzuki,Y., Yamanaka,A. and Tominaga,M. (2014) Modulation of water efflux through functional interaction between TRPV4 and TMEM16A/anoctamin 1. *FASEB J.*, **28**, 2238–2248.
https://doi.org/10.1096/fj.13-243436
http://www.ncbi.nlm.nih.gov/pubmed/24509911

16. Mendoza,S.A., Fang,J., Gutterman,D.D., Wilcox,D.A., Bubolz,A.H., Li,R., Suzuki,M. and Zhang,D.X. (2010) TRPV4-mediated endothelial Ca $^{2+}$ influx and vasodilation in response to shear stress. *Am. J. Physiol. Circ. Physiol.*, **298**, H466–H476.
https://doi.org/10.1152/ajpheart.00854.2009
http://www.ncbi.nlm.nih.gov/pubmed/19966050

17. Matsusaka,T. and Ichikawa,I. (1997) BIOLOGICAL FUNCTIONS OF ANGIOTENSIN AND ITS RECEPTORS. *Annu. Rev. Physiol.*, **59**, 395–412.
https://doi.org/10.1146/annurev.physiol.59.1.395

18. Mizuno,N. and Itoh,H. (2009) Functions and Regulatory Mechanisms of Gq-Signaling Pathways. *Neurosignals*, **17**, 42–54.
https://doi.org/10.1159/000186689
http://www.ncbi.nlm.nih.gov/pubmed/19212139

19. Kroeze,W.K., Sassano,M.F., Huang,X.-P., Lansu,K., McCorvy,J.D., Giguère,P.M., Sciaky,N. and Roth,B.L. (2015) PRESTO-Tango as an open-source resource for interrogation of the druggable human GPCRome. *Nat. Struct. Mol. Biol.*, **22**, 362–9.
https://doi.org/10.1038/nsmb.3014
http://www.ncbi.nlm.nih.gov/pubmed/25895059

20. Bihzad,S.M. and Yousif,M.H.M. (2017) 11,12-Epoxyeicosatrienoic acid induces vasodilator response in the rat perfused mesenteric vasculature. *Auton. Autacoid Pharmacol.*, **37**, 3–12.
https://doi.org/10.1111/aap.12052
http://www.ncbi.nlm.nih.gov/pubmed/28332266

21. Zhao,L., Sullivan,M.N., Chase,M., Gonzales,A.L. and Earley,S. (2014) Calcineurin/Nuclear Factor of Activated T Cells–Coupled Vanilliod Transient Receptor Potential Channel 4 Ca $^{2+}$

Sparklets Stimulate Airway Smooth Muscle Cell Proliferation. *Am. J. Respir. Cell Mol. Biol.*, **50**, 1064–1075.
https://doi.org/10.1165/rcmb.2013-0416OC
http://www.ncbi.nlm.nih.gov/pubmed/24392954

22. Masuyama,R., Vriens,J., Voets,T., Karashima,Y., Owsianik,G., Vennekens,R., Lieben,L., Torrekens,S., Moermans,K., Vanden Bosch,A., *et al.* (2008) TRPV4-Mediated Calcium Influx Regulates Terminal Differentiation of Osteoclasts. *Cell Metab.*, **8**, 257–265.
https://doi.org/10.1016/J.CMET.2008.08.002

23. Boddeke,H.W., Hoffman,B.J., Palacios,J.M. and Hoyer,D. (1993) Calcineurin inhibits desensitization of cloned rat 5-HT1C receptors. *Naunyn. Schmiedebergs. Arch. Pharmacol.*, **348**, 221–4.
http://www.ncbi.nlm.nih.gov/pubmed/7694158

24. Sanders-Bush,E. and Breeding,M. (1991) Choroid plexus epithelial cells in primary culture: a model of 5HT1C receptor activation by hallucinogenic drugs. *Psychopharmacology (Berl).*, **105**, 340–6.
http://www.ncbi.nlm.nih.gov/pubmed/1665919

25. Crabtree,G.R. (2001) Calcium, calcineurin, and the control of transcription. *J. Biol. Chem.*, **276**, 2313–6.
https://doi.org/10.1074/jbc.R000024200
http://www.ncbi.nlm.nih.gov/pubmed/11096121

26. Swingle,M., Ni,L. and Honkanen,R.E. (2007) Small-molecule inhibitors of ser/thr protein phosphatases: specificity, use and common forms of abuse. *Methods Mol. Biol.*, **365**, 23–38.
https://doi.org/10.1385/1-59745-267-X:23
http://www.ncbi.nlm.nih.gov/pubmed/17200551

27. Klee,C.B., Crouch,T.H. and Krinks,M.H. (1979) Calcineurin: a calcium- and calmodulin-binding protein of the nervous system. *Proc. Natl. Acad. Sci. U. S. A.*, **76**, 6270–3.
http://www.ncbi.nlm.nih.gov/pubmed/293720

28. Damkier,H.H., Brown,P.D. and Praetorius,J. (2013) Cerebrospinal Fluid Secretion by the Choroid Plexus. *Physiol. Rev.*, **93**, 1847–1892.
https://doi.org/10.1152/physrev.00004.2013
http://www.ncbi.nlm.nih.gov/pubmed/24137023

29. Orlandi,C., Cao,Y. and Martemyanov,K.A. (2013) Orphan receptor GPR179 forms macromolecular complexes with components of metabotropic signaling cascade in retina ON-bipolar neurons. *Invest. Ophthalmol. Vis. Sci.*, **54**, 7153–61.
https://doi.org/10.1167/iovs.13-12907
http://www.ncbi.nlm.nih.gov/pubmed/24114537

30. Vinuela-Fernandez,I., Sun,L., Jerina,H., Curtis,J., Allchorne,A., Gooding,H., Rosie,R., Holland,P., Tas,B., Mitchell,R., *et al.* (2014) The TRPM8 channel forms a complex with the 5-HT1B receptor and phospholipase D that amplifies its reversal of pain hypersensitivity. *Neuropharmacology*, **79**, 136–151.
https://doi.org/10.1016/j.neuropharm.2013.11.006
http://www.ncbi.nlm.nih.gov/pubmed/24269608

31. Chen,J. and Hackos,D.H. (2015) TRPA1 as a drug target--promise and challenges. *Naunyn. Schmiedebergs. Arch. Pharmacol.*, **388**, 451–63.
https://doi.org/10.1007/s00210-015-1088-3
http://www.ncbi.nlm.nih.gov/pubmed/25640188

32. Vetter,I., Wyse,B.D., Monteith,G.R., Roberts-Thomson,S.J. and Cabot,P.J. (2006) The mu opioid agonist morphine modulates potentiation of capsaicin-evoked TRPV1 responses through a cyclic AMP-dependent protein kinase A pathway. *Mol. Pain*, **2**, 22.
https://doi.org/10.1186/1744-8069-2-22
http://www.ncbi.nlm.nih.gov/pubmed/16842630

33. Majerus,P.W. (1992) Inositol Phosphate Biochemistry. *Annu. Rev. Biochem.*, **61**, 225–250.
https://doi.org/10.1146/annurev.bi.61.070192.001301

34. Kusudo,T., Wang,Z., Mizuno,A., Suzuki,M. and Yamashita,H. (2012) TRPV4 deficiency increases skeletal muscle metabolic capacity and resistance against diet-induced obesity. *J. Appl. Physiol.*, **112**, 1223–1232.
https://doi.org/10.1152/japplphysiol.01070.2011

35. Bahouth,S.W., Gokmen-Polar,Y., Coronel,E.C. and Fain,J.N. (1996) Enhanced desensitization and phosphorylation of the beta 1-adrenergic receptor in rat adipocytes by peroxovanadate. *Mol. Pharmacol.*, **49**.

36. Segal,M.B. (2000) The Choroid Plexuses and the Barriers Between the Blood and the Cerebrospinal Fluid. *Cell. Mol. Neurobiol.*, **20**, 183–196.
https://doi.org/10.1023/A:1007045605751

37. Preston,D., Simpson,S., Halm,D., Hochstetler,A., Schwerk,C., Schroten,H. and Blazer-Yost,B.L. (2018) Activation of TRPV4 stimulates transepithelial ion flux in a porcine choroid plexus cell line. *Am. J. Physiol. Physiol.*, **315**, C357–C366.
https://doi.org/10.1152/ajpcell.00312.2017
http://www.ncbi.nlm.nih.gov/pubmed/29791207

38. Hannan,M.A., Kabbani,N., Paspalas,C.D. and Levenson,R. (2008) Interaction with dopamine D2 receptor enhances expression of transient receptor potential channel 1 at the cell surface. *Biochim. Biophys. Acta*, **1778**, 974–82.
https://doi.org/10.1016/j.bbamem.2008.01.011
http://www.ncbi.nlm.nih.gov/pubmed/18261457

39. Gáborik,Z., Jagadeesh,G., Zhang,M., Spät,A., Catt,K.J. and Hunyady,L. (2003) The Role of a Conserved Region of the Second Intracellular Loop in AT $_1$ Angiotensin Receptor Activation and Signaling. *Endocrinology*, **144**, 2220–2228.
https://doi.org/10.1210/en.2002-0135
http://www.ncbi.nlm.nih.gov/pubmed/12746278

40. Arniges,M., Fernández-Fernández,J.M., Albrecht,N., Schaefer,M. and Valverde,M.A. (2006) Human TRPV4 Channel Splice Variants Revealed a Key Role of Ankyrin Domains in Multimerization and Trafficking. *J. Biol. Chem.*, **281**, 1580–1586.
https://doi.org/10.1074/jbc.M511456200
http://www.ncbi.nlm.nih.gov/pubmed/16293632

41. Meixiong,J., Vasavda,C., Green,D., Zheng,Q., Qi,L., Kwatra,S.G., Hamilton,J.P., Snyder,S.H. and Dong,X. (2019) Identification of a bilirubin receptor that may mediate a component of cholestatic itch. *Elife*, **8**.
https://doi.org/10.7554/eLife.44116

42. Violin,J.D., Ren,X.-R. and Lefkowitz,R.J. (2006) G-protein-coupled Receptor Kinase Specificity for β-Arrestin Recruitment to the β_2 -Adrenergic Receptor Revealed by Fluorescence Resonance Energy Transfer. *J. Biol. Chem.*, **281**, 20577–20588.
https://doi.org/10.1074/jbc.M513605200
http://www.ncbi.nlm.nih.gov/pubmed/16687412

43. Hughes,T.E., Zhang,H., Logothetis,D.E. and Berlot,C.H. (2001) Visualization of a Functional $G\alpha_q$ -Green Fluorescent Protein Fusion in Living Cells. *J. Biol. Chem.*, **276**, 4227–4235.
https://doi.org/10.1074/jbc.M007608200
http://www.ncbi.nlm.nih.gov/pubmed/11076942

44. Boehm,J.S., Zhao,J.J., Yao,J., Kim,S.Y., Firestein,R., Dunn,I.F., Sjostrom,S.K., Garraway,L.A., Weremowicz,S., Richardson,A.L., *et al.* (2007) Integrative Genomic Approaches Identify IKBKE as a Breast Cancer Oncogene. *Cell*, **129**, 1065–1079.
https://doi.org/10.1016/j.cell.2007.03.052
http://www.ncbi.nlm.nih.gov/pubmed/17574021

45. Zhang,D.X., Mendoza,S.A., Bubolz,A.H., Mizuno,A., Ge,Z.-D., Li,R., Warltier,D.C., Suzuki,M. and Gutterman,D.D. (2009) Transient receptor potential vanilloid type 4-deficient mice exhibit impaired endothelium-dependent relaxation induced by acetylcholine in vitro and in vivo. *Hypertens. (Dallas, Tex. 1979)*, **53**, 532–8.
https://doi.org/10.1161/HYPERTENSIONAHA.108.127100
http://www.ncbi.nlm.nih.gov/pubmed/19188524

46. Monnot,A.D. and Zheng,W. (2012) Culture of Choroid Plexus Epithelial Cells and In Vitro Model of Blood–CSF Barrier. In *Methods in molecular biology (Clifton, N.J.)*.Vol. 945, pp. 13–29.
https://doi.org/10.1007/978-1-62703-125-7_2
http://www.ncbi.nlm.nih.gov/pubmed/23097098

47. Vasavda,C., Zaccor,N.W., Scherer,P.C., Sumner,C.J. and Snyder,S.H. (2017) Measuring g-protein-coupled receptor signaling via radio-labeled GTP binding. *J. Vis. Exp.*, **2017**.
https://doi.org/10.3791/55561

48. Thomas,W.G. (2009) G Protein-Coupled Receptors in Drug Discovery Vol. 552. Leifert,W.R. (ed) Humana Press.
https://doi.org/10.1007/978-1-60327-317-6_26

FOOTNOTES

This work was supported by the US National Institutes of Health: DA044123-1A1 (SHS), MH018501-48 (SHS), MH100024-05 (SHS), NS062869 (CJS), NS087579 (CJS), OD016374 (S. Kuo) and GM007309 (NWZ).

The abbreviations used are: TRPV4, transient receptor potential vanilloid 4; AT1R, angiotensin II receptor type 1; GPCR, G-protein coupled receptor; ANGII, angiotensin II; TRP, transient receptor potential; cAMP, cyclic adenosine monophosphatase; IP3, inositol trisphosphate; DAG, diacyl glycerol; PLC, phospholipase C; GRK, g-protein receptor kinase; MAPK, mitogen activated protein kinase; rVSMC, rat vascular smooth muscle cell; MOR1, μ-opiod receptor 1; TRPC1, transient receptor potential canonical 1; TRPC3, transient receptor potential canonical 3; TRPM8, transient receptor potential melanostatin 8; mGluR1, metabotropic glutamate receptor 1; TRPV1, transient receptor potential vanilloid 1; 11,12 EET, 11,12-Epoxyeicosatrienoic acid; CPEC, choroid plexus epithelial cell; CSF, cerebrospinal fluid; NFAT, nuclear factor of activated T-cells; Co-IP, co-immunoprecipitate; PD, pull down; WT, wild type; KO, knockout; IF, immunofluorescence; HPLC, high pressure liquid chromoatography.

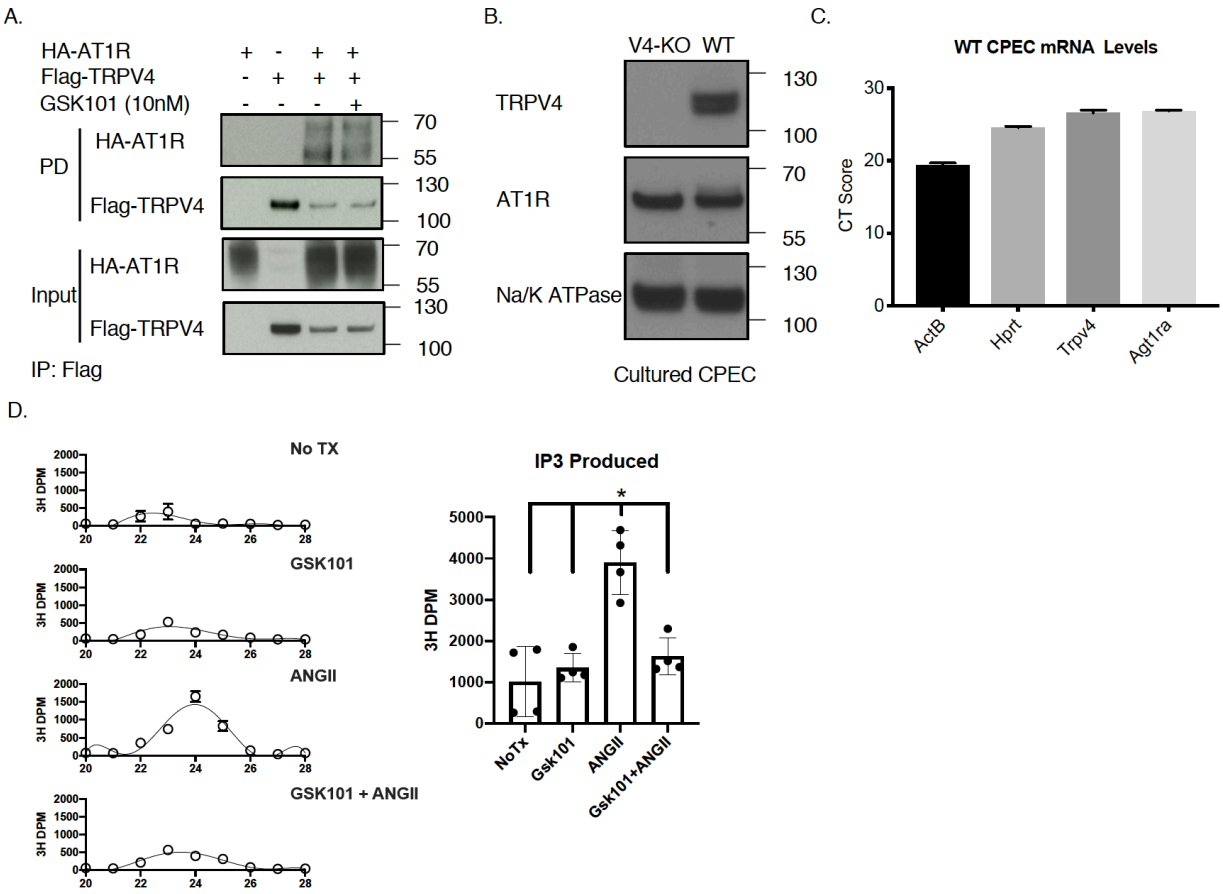

Figure 1. TRPV4 and AT1R are co-expressed in the same tissue, bind to one another and interact physiologically. (A) Flag-TRPV4 and HA-AT1R co-IP in transiently transfected HEK293 cells whether or not treated with 10 nM GSK101. GSK101 was applied for 10 min pre-lysis. (B) Western blot from CPECs from WT and TRPV4-KO . WT CPECs express both AT1R and TRPV4. TRPV4-KO CPECs express AT1R and no TRPV4. (C) RT-qPCR of mRNA extracted from CPECs from WT mice. Error bars denote mean ± SD. (D) Left: IP3 production measured using HPLC from HEK293 cells expressing TRPV4 and AT1R. Cells were stimulated with combinations of 10nM GSK101 for 10 min and 100nM ANGII for 2 min. Right: Total IP3 is measured by calculating the area under the curve for elution fractions #21-#27. n = 4. Error bars denote mean ± SD. * $p < 0.05$. Pulldown westerns indicated by PD. CPECs cultured for 12 days *in vitro* prior to experimentation.

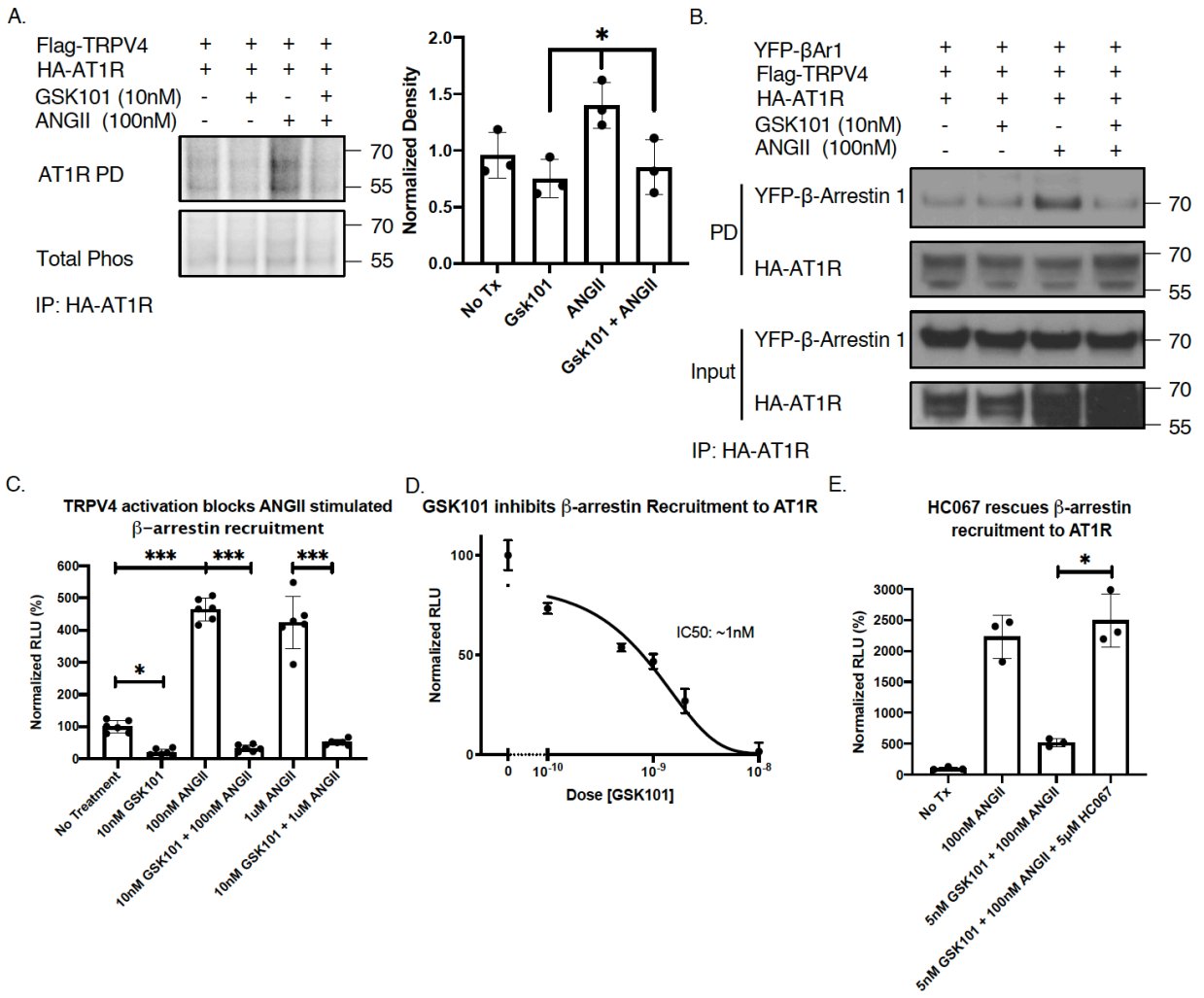

Figure 2. TRPV4 inhibits ligand induced AT1R phosphorylation and subsequent β-arrestin recruitment. (A) Left: Autoradiograph from IP for HA from HEK293 cells overexpressing HA-AT1R and Flag-TRPV4. HEK293 cells were incubated in [32P]-orthophosphate and stimulated with indicated combinations of 100nM ANGII for 10 min and 10 nM GSK101 for 5 min. Right: Densitometry quantification of phosphorylated band normalized to total phosphorylated protein. n=3. (B) HEK293 cells overexpressing HA-AT1R, Flag-TRPV4 and YFP-β-arrestin 1 were treated with indicated drug combinations of 10 nM GSK101 and 100 nM ANGII for 10 min and 20 min respectively. IP indicates immunoprecipitation with HA primary and blot for HA and YFP pull down. (C - E) HTLA cells expressing Flag-TRPV4 and AT1R-Tango stimulated with GSK101 and ANGII for 10 min and 30 min respectively (C) Normalized luciferase production stimulated with indicated drug combinations. n = 6. (D) Normalized luciferase production stimulated by 100 nM ANGII and increasing doses of GSK101. n = 3. (E) Normalized luciferase production in response to combinations of 100 nM ANGII and 5 nM GSK101 in the presence and absence of 5 μM HC067, a TRPV4 antagonist. n = 3. All error bars denote mean ± SD. All graphs analyzed by one-way ANOVA corrected for multiple comparisons with a *post hoc* Tukey Test. * $p < 0.05$, *** $p<0.0005$. Normalization described in methods.

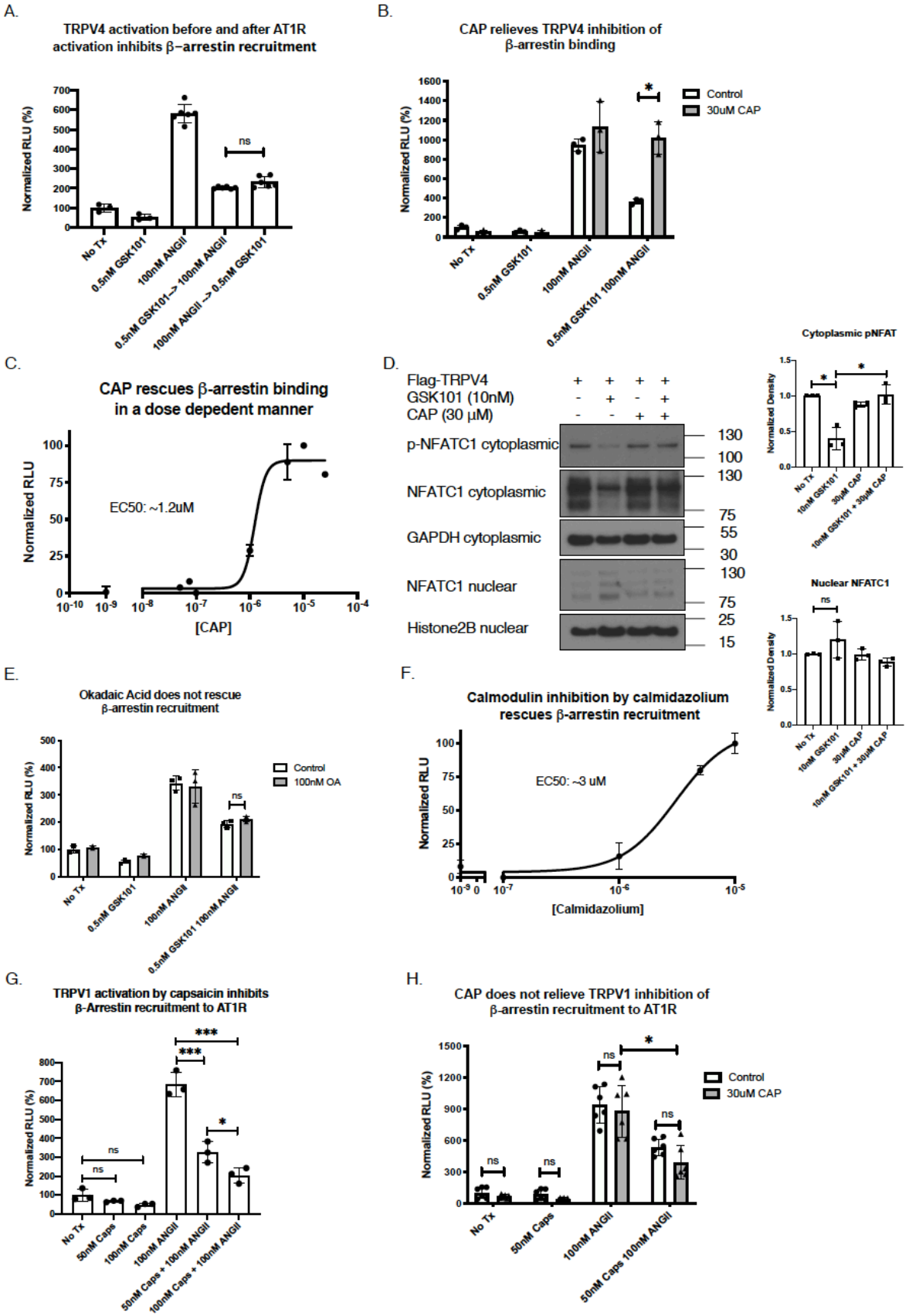

Figure 3. TRPV4 activates calcineurin to dephosphorylate AT1R receptor in a Ca2+/Calmodulin dependent manner. (A – C) HTLA cells expressing Flag-TRPV4 and AT1R-Tango stimulated with GSK101 for 10 min and ANGII for 30 min. (A) Normalized luciferase production in response to activating AT1R before or after TRPV4 activation, n = 3-6. (B) Normalized luciferase production in response to AT1R and TRPV4 activation in the presence of 30 μM CAP, n = 3. (C) Normalized luciferase production in response to 0.5 nM GSK101 stimulation followed by 100 nM ANGII stimulation in the presence of increasing concentrations of CAP, n = 3. (D) Left: Cell fractionation and immunoblotting to determine subcellular localization of p-NFATC1 and NFATC1 in HEK293 cells expressing Flag-TRPV4. Cells treated with indicated doses of GSK101 for 10 min prior to lysis. Right: Densitometry of cytoplasmic p-NFATC1 (Top) and nuclear NFATC1 (bottom). GAPDH is a cytoplasmic protein loading control. Histone 2B is a nuclear protein loading control. (E - F) HTLA cells expressing Flag-TRPV4 and AT1R-Tango stimulated with GSK101 for 10 min and ANGII for 30 min. (E) Normalized luciferase production in response to activating TRPV4 with 0.5 nM GSK101 for 10 min followed by activating AT1R with 100 nM ANGII for 30 min in the presence or absence of 100nM Okadaic Acid, n = 3. (F) Normalized luciferase production in response to 0.5 nM GSK101 stimulation followed by 100 nM ANGII stimulation in the presence of increasing concentrations of calmidazolium, calmodulin inhibitor, n = 3. (G-H) HTLA cells expressing Flag-TRPV1 and AT1R-Tango stimulated with 50 nM capsaicin for 10 min and 100 nM ANGII for 30 min. (G) Normalized luciferase production in response to TRPV1 and AT1R activation. (H) Normalized luciferase production in response to AT1R and TRPV1 activation in the presence of 30 μM CAP, n = 6. All error bars denote mean ± SD. All graphs analyzed by one-way ANOVA corrected for multiple comparisons with a *post hoc* Tukey Test. * $p < 0.05$, *** $p<0.005$.

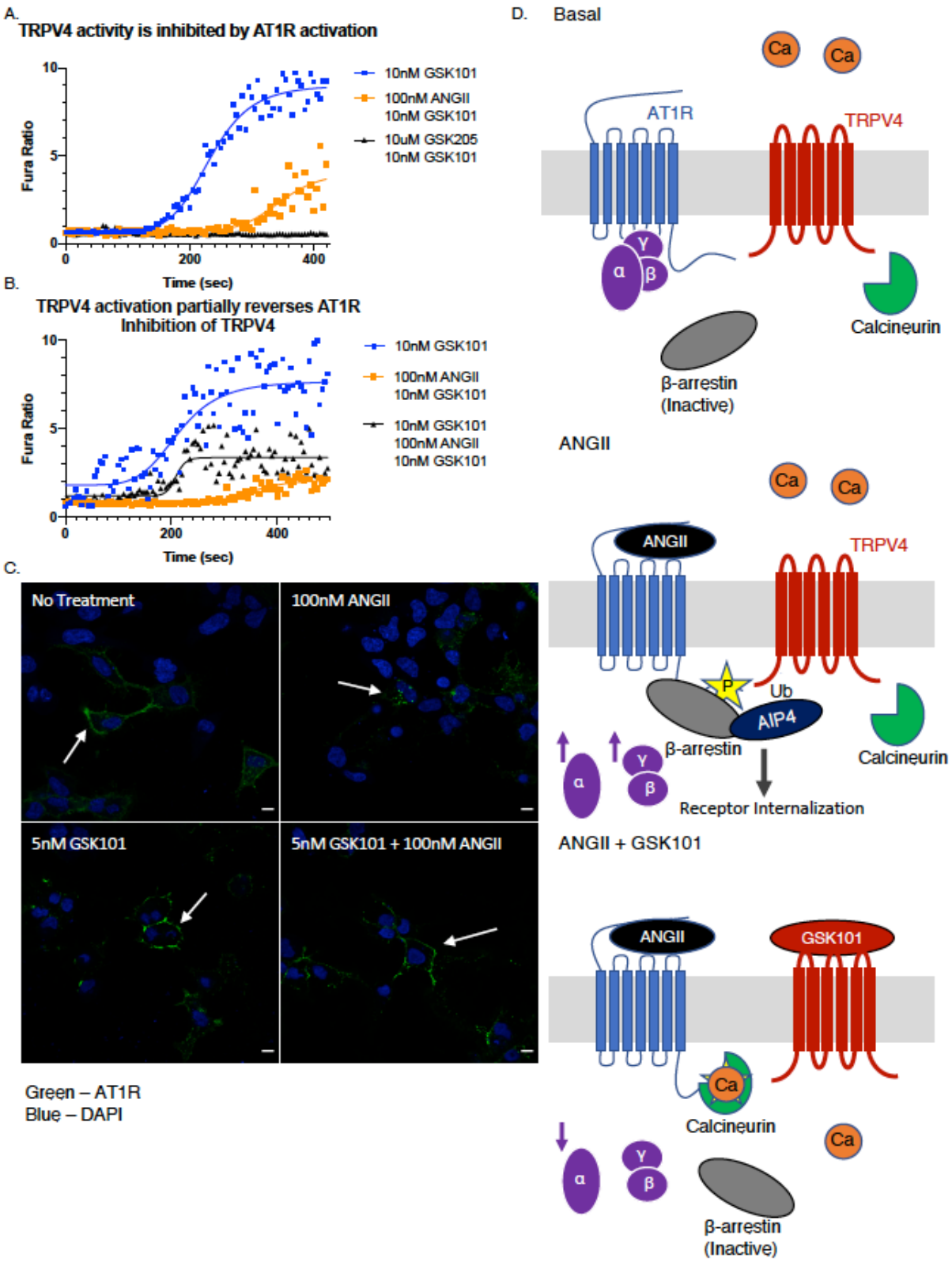

Figure 4. TRPV4 activity can be regulated by AT1R activation. (A – B) Calcium imaging of CPECs cultured for 12 days *in vitro*, cells are imaged only for the last 10nM GSK101 dose. (A) CPECs stimulated

with 10 nM GSK101 (Blue), 100 nM ANGII for 30 min followed by 10 nM GSK101 (Orange), and cells incubated in 10 μM GSK205 followed by 10 nM GSK101 (Black), n = 7-10. (B) CPECs stimulated with 10 nM GSK101 (Blue), 100 nM ANGII for 30 min followed by 10 nM GSK101 (Orange) and 10 nM GSK101 for 10 min, followed by 100 nM ANGII for 30 min and then 10 nM GSK101 a second time, n = 10-23. (C) IF of HEK293 cells expressing HA-AT1R and Flag-TRPV4 treated with indicated combinations 10 nM GSK101 and 100nM ANGII for 10 min and 20 min respectively. Primary antibody was added prior to drug applications. White arrows indicate specific locations on cells of interest. Green – HA-AT1R, Blue – Hoechst. Scale bar 10 μm. (D) Hypothetical schematic of the TRPV4 interaction with AT1R. Top: At baseline TRPV4 and AT1R are co-expressed in the same cell and may physically interact. Middle: ANGII mediated activation of AT1R catalyzes the activation of Gαq and βγ signaling, as well as recruits β-arrestin to bind its phosphorylated c-terminus. β-arrestin then mediates ubiquitination of TRPV4 by AIP4. Bottom: TRPV4 activation activates calcineurin in Ca2+/Calmodulin dependent manner, which dephosphorylates AT1R, inhibiting recruitment of β-arrestin, and therefor inhibiting internalization. Separately, TRPV4 activation inhibits Gαq signaling by reducing IP3 accumulation.

The nonselective cation channel TRPV4 inhibits angiotensin II receptors

Nicholas W. Zaccor, Charlotte J. Sumner and Solomon H. Snyder

J. Biol. Chem. published online June 3, 2020

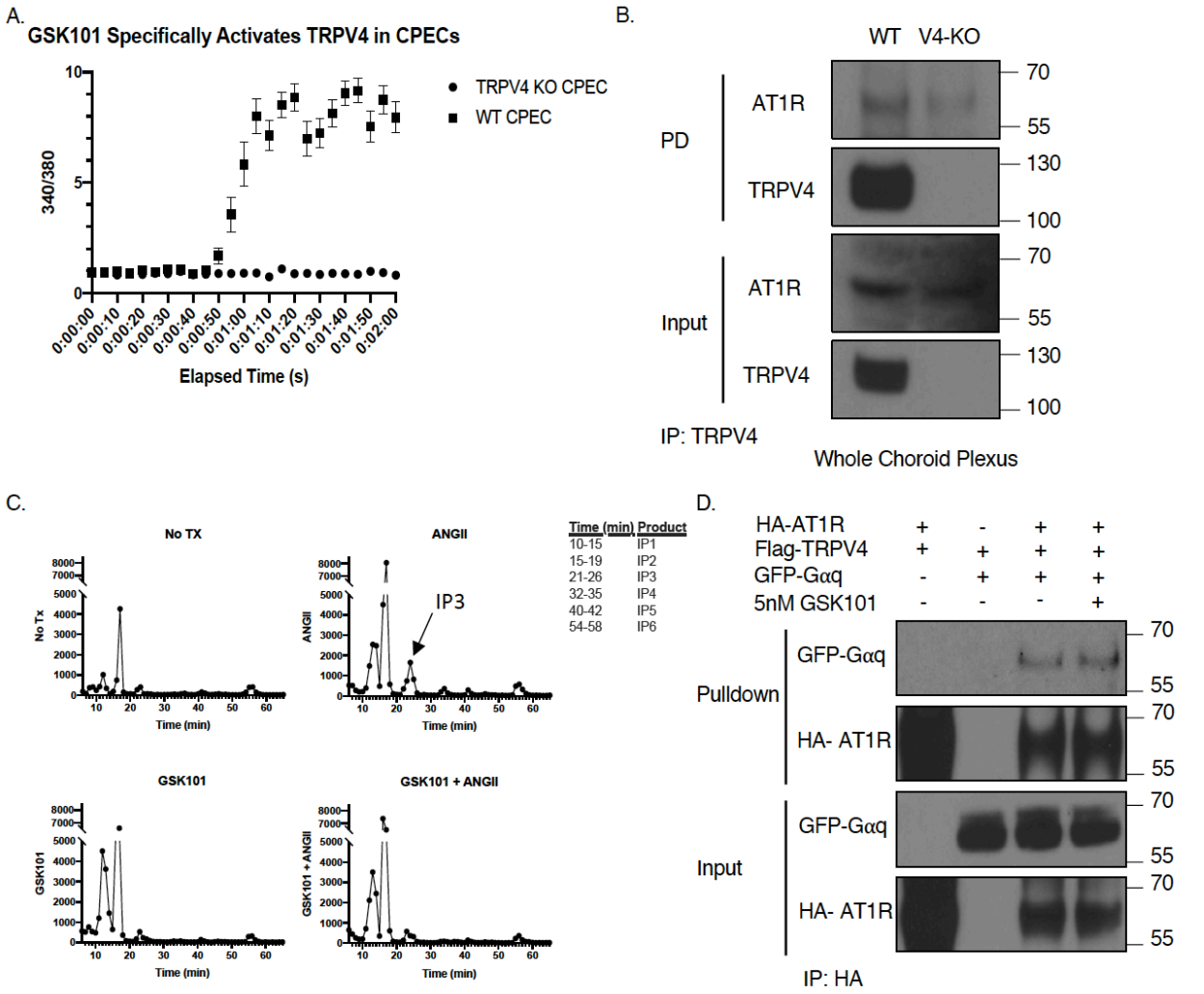

Supplemental Figure 1. TRPV4 is expressed in the choroid plexus and activated by GSK101. (A) Calcium imaging of WT and TRPV4-KO CPEC treated with 10 μM GSK101. n = 4. (B) AT1R co-IPs with TRPV4 from whole choroid plexus from WT, but poorly in TRPV4-KO mice. (C) HPLC curve of all phosphorylated inositol isoforms for HEK293 cells transiently expressing Flag-TRPV4 and HA-AT1R treated with combinations of 10nM GSK101 for 5 min and 100nM ANGII for 2 min, n= 4. IP3 peak indicated by arrow. Legend indicates which elution fractions are associated with each inositol isoform. All error bars denote mean ± SD. (D) IP of HA-AT1R from cells overexpressing indicated combinations of HA-AT1R, Flag-TRPV4 and GFP-Gαq. Immunoblot for HA and GFP. Cells treated with 5nM GSK101 for 10 min prior to lysis.

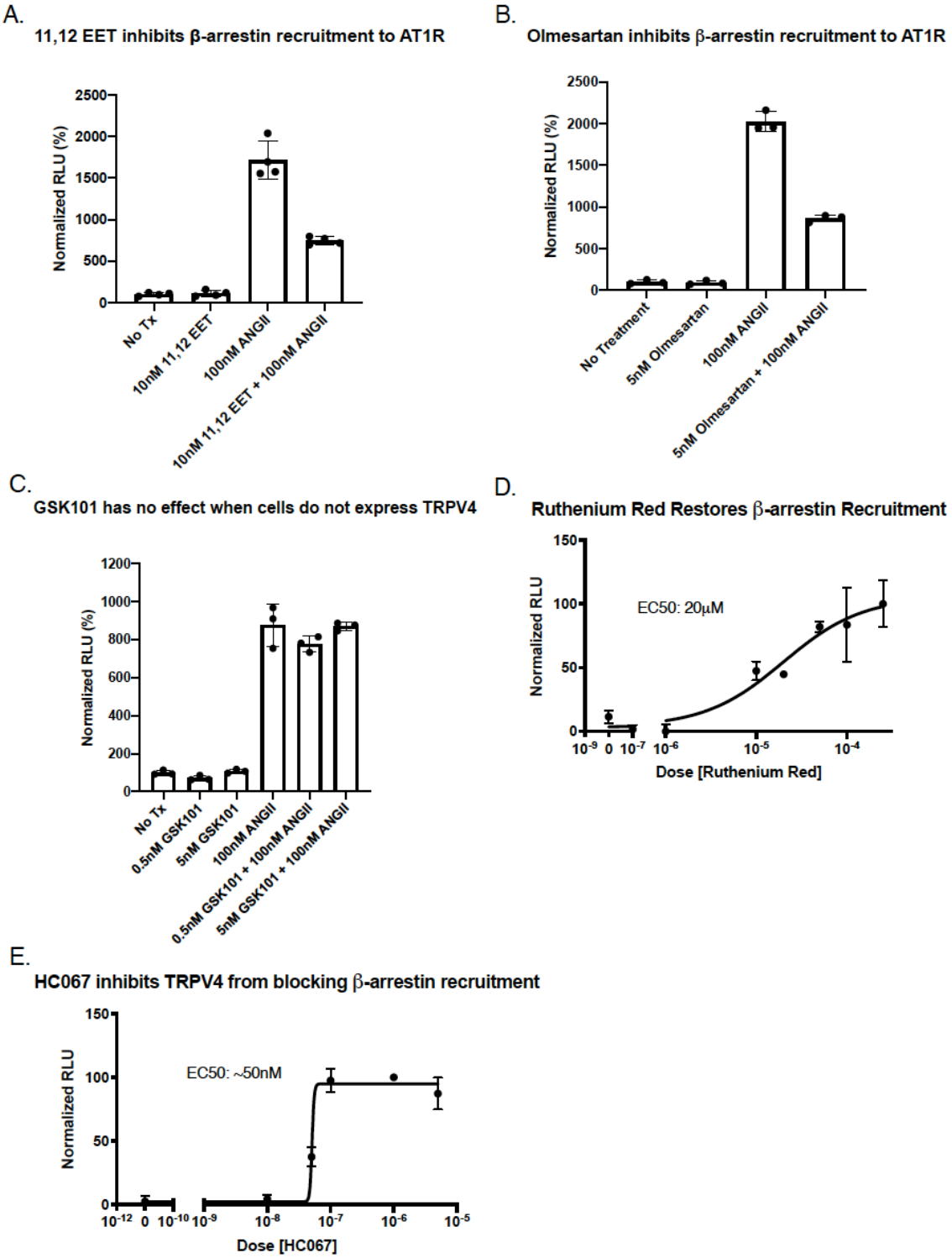

Supplemental Figure 2. TRPV4 activation blocks arrestin recruitment, which can be rescued by TRPV4 inhibition. (A) HTLA cells co-expressing Flag-TRPV4 and AT1R-Tango. Luciferase production stimulated by treatment with combinations of 10 nM 11,12 EET for 10 min and 100 nM ANGII for 30 min, n = 4. (B)

HTLA cells expressing Flag-TRPV4 and AT1R-Tango. Cells were treated with 100 nM ANGII for 30 min in the presence of absence of 5 nM Olmesartan, an AT1R inverse agonist. (C) HTLA cell expressing AT1R-Tango and no TRPV4. Luciferase production stimulated by treatment with combinations of 0.5 nM or 5 nM GSK101 and 100 nM ANGII for 10 min and 30 min respectively, n = 3. (D-E) HTLA cells co-expressing Flag-TRPV4 and AT1R-Tango. Luciferase production stimulated by treatment with 1 nM GSK101 for 10 min and 100 nM ANGII for 30 min in the presence of increasing doses of (D) Ruthenium red, EC50 = ~20 μM, n=3 and (E) HC067, EC50 = ~50nM, n=3. All error bars denote mean ± SD.

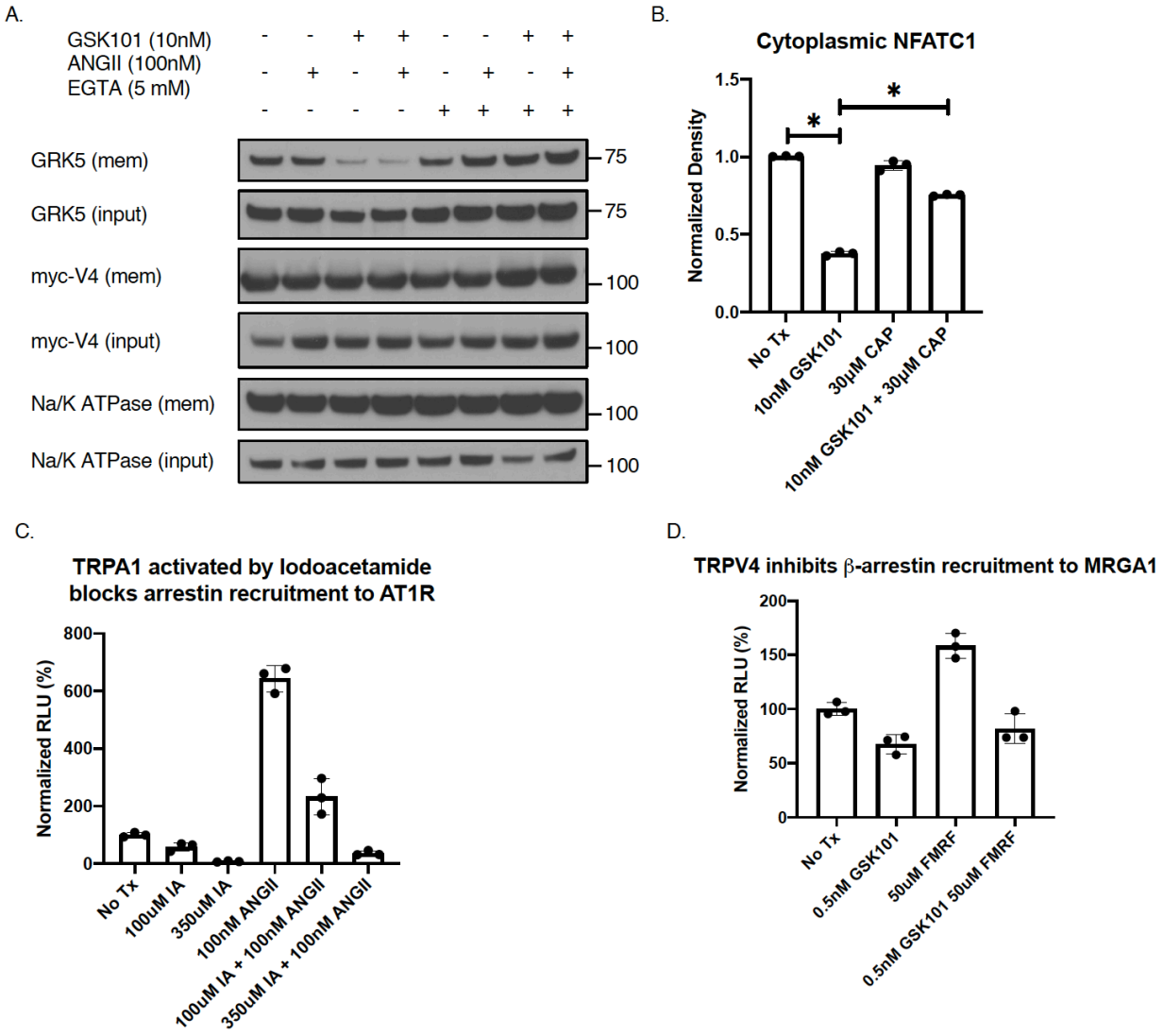

Supplemental Figure 3. TRP channels may generally inhibit G-protein kinase 5 and block arrestin recruitment. (A) Immunoblot of membrane proteins isolated from HEK293 cells transiently expressing Flag-GRK5, myc-TRPV4, and HA-AT1R. Cells were treated with indicated combinations of 10 nM GSK101 for 10 min and 100 nM ANGII for 10 min indicated in the figure in the presence and absence of 5 mM EGTA. (B) Densitometry of cytoplasmic NFATC1. Cell fractionation and immunoblotting to determine subcellular localization of endogenous p-NFATC1 and NFATC1 in HEK293 cells expressing Flag-TRPV4. (C) HTLA cells transiently expressing Flag-TRPA1 and AT1R-Tango. Luciferase production stimulated by combinations of 100 μM or 350 μM IA, a TRPA1 agonist, for 10 min and 100 nM ANGII for 30 min, n = 3. (D) HTLA cells expressing Flag-TRPV4 and MRGA1-Tango. Luciferase production

stimulated by combinations of 0.5 nM GSK101 for 10 min and 50 μM FMRF, a MRGA1 agonist, for 30 min, n = 3. Error bars denote mean ± SD.

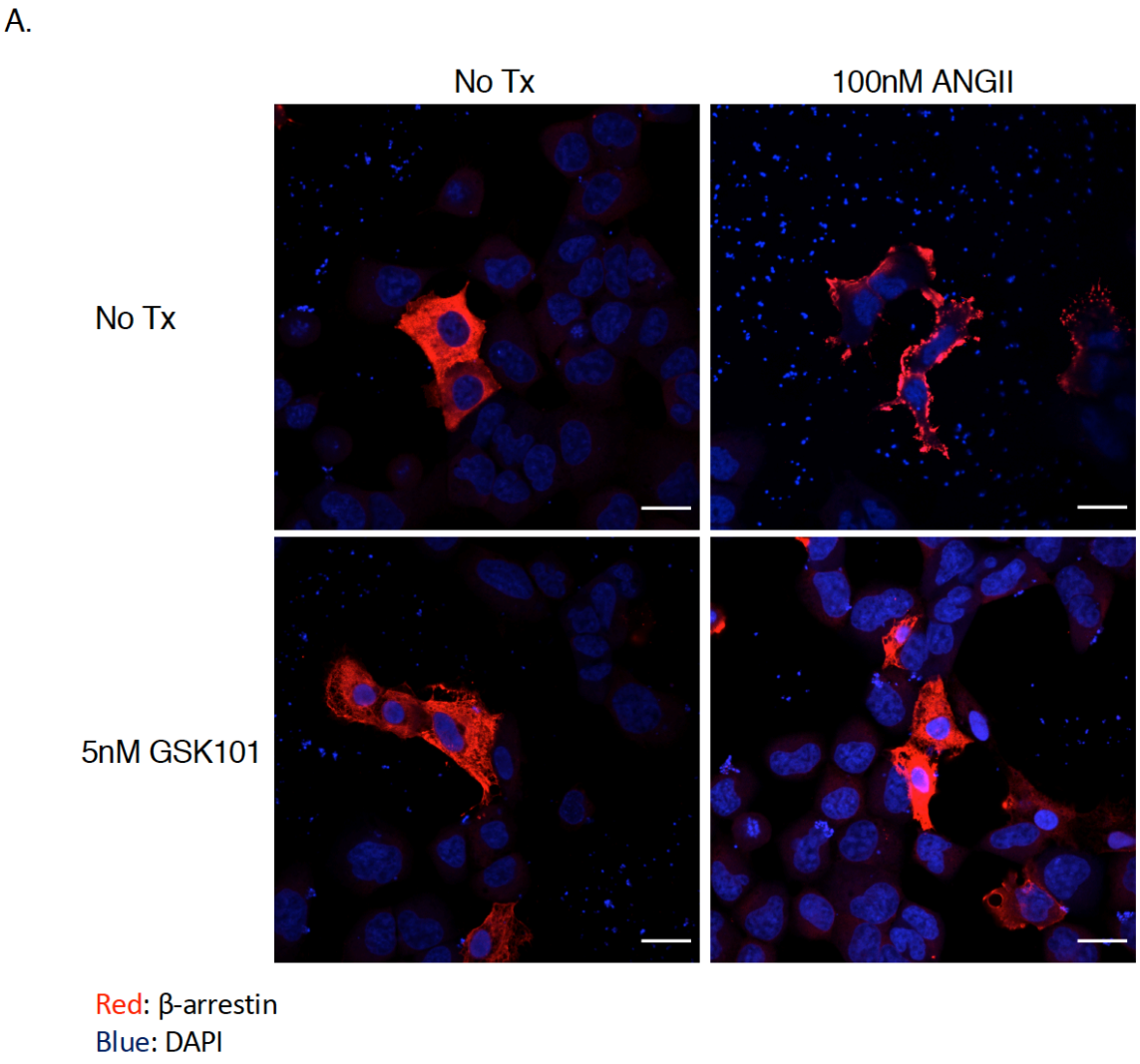

Supplemental Figure 4. β-arrestin recruitment to the cell membrane is inhibited by activating TRPV4. (A) HTLA cells transiently overexpressing Flag-TRPV4, HA-AT1R and YFP-β-arrestin 1. Cells were treated with indicated combinations of 5nM GSK101 for 10 min and then 100nM ANGII for 7 min. β-arrestin – red, DAPI – blue. Scale bar = 25μM.